PHYSICAL REVIEW B **68**, 024429 (2003)

Charge disproportionation in $YNiO_3$: ESR and susceptibility study

M. T. Causa,* R. D. Sánchez, and M. Tovar
Centro Atómico Bariloche, CNEA, Av. Ezequiel Bustillo 9500, (8400) San Carlos de Bariloche, Río Negro, Argentina

J. A. Alonso and M. J. Martínez-Lope
Instituto de Ciencia de Materiales de Madrid, CSIC, Cantoblanco, E-28049 Madrid, Spain

(Received 22 October 2002; revised manuscript received 8 May 2003; published 30 July 2003)

We present a study of the magnetic properties of $YNiO_3$ in the paramagnetic range above and below the metal-insulator (MI) transition. The dc susceptibility χ_{dc} (measured up to 1000 K) is a decreasing function of T for $T > 150$ K (the Néel temperature) and we observe two different Curie-Weiss regimes corresponding to the metallic and insulating phases. In the metallic phase, this behavior seems to be associated with the small ionic radius of Y^{3+}. An electron spin resonance (ESR) spectrum compatible with Ni^{2+} is visible in the insulating phase but only a fraction of the Ni ions contributes to this resonance. We explain the ESR and χ_{dc} behavior for $T < T_{MI}$ in terms of charge disproportionation of the type $2Ni^{3+} \rightarrow Ni^{2+} + Ni^{4+}$, associated with the previously observed structural transition across T_{MI}. Effects of thermally excited electronic configurations on χ_{dc} are discussed.

DOI: 10.1103/PhysRevB.68.024429 PACS number(s): 75.30.Cr, 71.30.+h, 71.45.Lr, 76.30.−v

I. INTRODUCTION

The perovskite system RNiO$_3$ (with R trivalent rare earth or Y) is a very attractive family of compounds around which an intense research activity was developed in the 1990s. Their most studied property was the metal-insulator (MI) transition[1] at T_{MI}, from a high-temperature metallic material to a charge-transfer insulator. As is seen in the phase diagram of Fig. 1, T_{MI} increases as the ionic radius of R^{3+} (r_R) diminishes. In the insulating phase the oxides show a complex antiferromagnetic (AFM) order, below a Néel temperature (T_N) also dependent on r_R. In spite of all the performed studies, the nature of the MI transition is not completely understood[2] and a model describing structural, magnetic, and transport properties for the whole RNiO$_3$ series is still lacking. The difficulties found in the synthesis of RNiO$_3$ are more severe for the smaller-r_R compounds[2,3] and only recently,[4] with new synthesis techniques, samples with R = Dy, Y, Ho, Er, and Lu could be studied. Besides, synchrotron x-ray diffraction (SXRD) techniques have allowed a more precise description of the structural changes[2] accompanying the MI transition.

In this paper we present a magnetic study of $YNiO_3$. Due to the nonmagnetic character of Y, the properties of the Ni lattice can be analyzed above and below T_{MI} without interference with other magnetic species. Notice that $LaNiO_3$, where La is also nonmagnetic, was found[5] to be metallic for all $T \geqslant 1.4$ K. Alonso *et al.*[2] have determined the MI transition for $YNiO_3$ at $T_{MI} = 582$ K. They observed a structural transition from the orthorhombic *Pbnm* phase (above T_{MI}) to a monoclinic $P21/n$ phase (below T_{MI}). This transition was compatible with a charge disproportionation in the insulating phase[2,4] where $2Ni^{3+} \rightarrow Ni^{3+\delta} + Ni^{3-\delta}$ ($\delta \approx 0.35$). In this interpretation, the two Ni species are localized in two different crystalline sites characterized by expanded (Ni1 site) and contracted (Ni2 site) NiO$_6$ octahedra. The AFM spin configuration below T_N was determined by neutron diffraction,[2] finding different magnetic moments associated with the two Ni sites. In this work we study the T dependence of the electron spin resonance (ESR) and the magnetic susceptibility. Our aim is to describe the changes in the magnetic properties associated with the MI transition. We discuss our results considering the effects of charge disproportionation and thermal population of the excited electron configurations.

II. EXPERIMENTAL DETAILS

Powder $YNiO_3$ samples were prepared under high-pressure and high-temperature conditions. A stoichiometric mixture of Y_2O_3 and $Ni(OH)_2$ powders was ground with 30% of $KClO_4$ and packed into an 8-mm-diam gold capsule placed in a cylindrical graphite heater. The reaction was carried out in a piston-cylinder press, under a pressure of 20 kbar at 1173 K for 20 min. The reaction product, in the form of blackish dense polycrystalline pellets, was ground and the resulting powder washed with water to dissolve KCl. The sample was characterized by x-ray diffraction. The magnetization $M(T)$ was measured with a superconducting quantum interference device (SQUID) magnetometer for $T < 300$ K and with a Faraday balance magnetometer in the range 250–1000 K. The ESR spectrum was measured with a Bruker ESP300 spectrometer operating at a frequency $\nu \approx 9.3$ GHz. We detected the derivative spectrum and determined the T dependence (up to 800 K) of the three ESR parameters: resonance field $H_0(T)$, peak-to-peak linewidth $\Delta H_{pp}(T)$, and double-integrated intensity $I_{ESR}(T)$. Notice that, alternatively, the intensity can be obtained[6] as $I_{ESR} = W[\Delta H_{pp})^2 \times h_{pp}]$ where h_{pp} is the height between peaks of the derivative spectrum and the constant W is dependent on the line shape ($W = 3.63$ for Lorentzian lines). This method was preferred to the double integration for low signal-to-noise ratio spectra in order to minimize possible spurious effects due to the cavity background. We took care to check the agreement between $I_{ESR}(T)$ derived in both ways in the region of good signal-to-noise ratio. The spec-

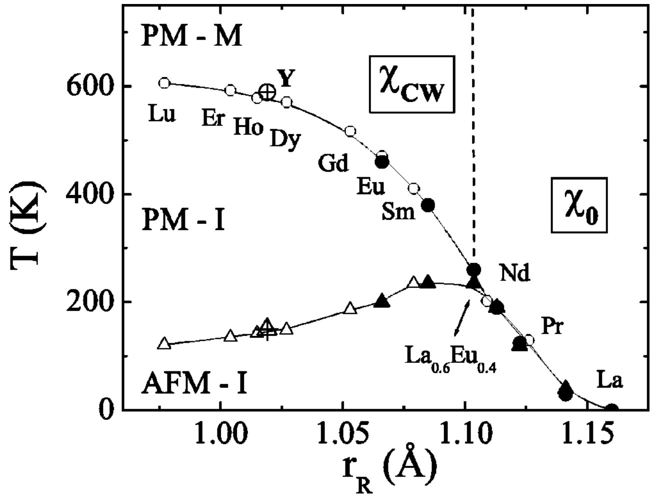

FIG. 1. T_{MI} (open circles) and T_N (open triangles) vs r_R for RNiO$_3$ (taken from Refs. 1 and 4). Crossed and solid symbols indicate, respectively, the results for YNiO$_3$ (present work) and for La$_{1-x}$Eu$_x$MnO$_3$ (Ref. 27). Solid lines are guides to the eye. The dashed line separates regions where T-dependent (χ_{CW}) and T-independent (χ_0) susceptibilities are observed in the metallic phase.

trum intensity was compared to that of well-characterized standard samples (MnF$_2$ single crystal and Gd$_2$ BaCuO$_5$ powder[7]) in order to determine the absolute value of the ESR susceptibility $\chi_{ESR}(T) \propto I_{ESR}(T)$, which is expected to be equal to $\chi_{dc}(T)$ if all the magnetic species contribute equally to the resonance. The detected lines were of relatively low intensity, and 100-mg samples were used in order to obtain low-noise spectra.

III. RESULTS AND DISCUSSION

In agreement with the pioneering experiment by Demazeau *et al.*,[3] $M(T)$ shows a peak at $T_N = 150$ K attributed to an AFM transition. Above T_N, $M(T)$ presents a paramagnetic (PM) behavior with $M(T) = \chi_{dc}(T)H$, where the susceptibility $\chi_{dc}(T)$, measured for $H = 10$ kG, follows a Curie-Weiss- (CW-) like law (see Fig. 2). In the ordered phase, $M(T)$ showed also a linear dependence on H (up to 50 kG) although with a very small extrapolated component $M_0 \simeq 10^{-4}\mu_B$/f.u., which saturates above $H \cong 1$ kG. This ferromagneticlike contribution may arise from uncompensated Ni moments or an imperfect AFM alignment. Besides, below ≈ 20 K an extra Curie contribution to $\chi_{dc}(T)$ is observed, as in other perovskites.[8,9] In our case, the smallness of the measured Curie constant $C = 0.003$ emu K/mol (YNiO$_3$) indicates that it could originate in impurities or defects and does not affect the results in the PM regime. This value for C would correspond to a minority phase of less than 0.03% (if the magnetism comes from rare-earth impurity ions) or at most $\approx 0.3\%$ (if it arises from paramagnetic Ni^{2+} ions). These level of impurities was not detected by XRD.

In the paramagnetic range ($T \geqslant T_N$), $\chi_{dc}(T)$ presents a small anomaly in the slope of $\chi_{dc}^{-1}(T)$ around T_{MI} (see inset of Fig. 2). For $T > T_{MI}$, a Curie constant $C = 0.79(2)$ emu K/mol and a CW temperature $\Theta = -210$ K were obtained. Below T_{MI}, $C = 0.90(2)$ emu K/mol and $\Theta = -310$ K. These values are larger than those derived by Demazeau *et al.*[3] from data obtained in the range 70–480 K. Notice that the crystalline parameters vary according to the preparation method: e.g., at room temperature the monoclinic angle $\beta = 90.08(1)°$ for the samples of Alonso *et al.*[4] and $\beta = 93.6°$ for the samples of Demazeau *et al.*[3]

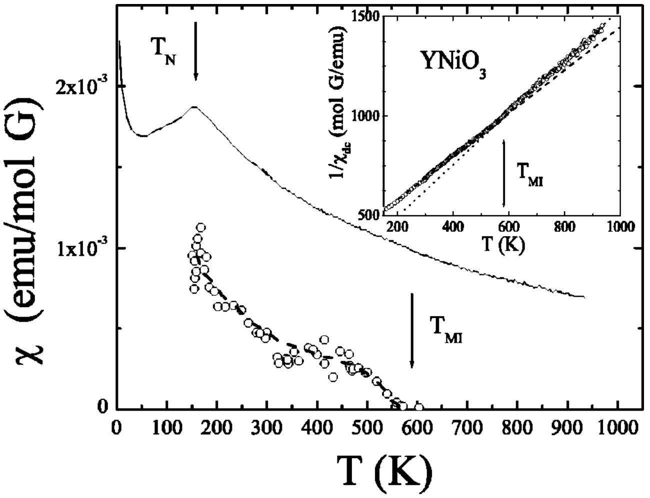

FIG. 2. Solid line: $\chi_{dc}(T)$. Circles: $\chi_{ESR}(T)$. The dashed line is a guide to the eye. In the inset $\chi_{dc}^{-1}(T)$ is plotted and the dashed (dotted) line is the fitting to a CW-like behavior for $T < T_{MI}$ ($T > T_{MI}$).

In the simplest ionic picture for the magnetic properties all Ni sites are equivalent and expected to be occupied by Ni^{3+} ions ($3d^7$). In the metallic states we may usually describe $\chi_{dc}(T)$ in terms of a sum of T-independent (χ_0) and a CW-like (χ_{CW}) susceptibilities[10] corresponding to itinerant and localized electrons, respectively. For RNiO$_3$ these would be the e_g and t_{2g}^6 electrons of low spin (LS) Ni^{3+}($t_{2g}^6 e_g^1$). Then, only a temperature-independent susceptibility χ_0 is expected for $T > T_{MI}$ since the localized t_{2g}^6 core has fully compensated spins. This behavior has been indeed observed[5] in LaNiO$_3$. Instead, as was mentioned above, we have measured a CW-like susceptibility for the metallic phase of YNiO$_3$ up to 1000 K, with a relatively large effective moment ($\mu_{eff} = 2.5\mu_B$). Within the same ionic picture, the MI transition occurs when the itinerant e_g electrons become localized. Here, again, the experimental results fail to validate this simple model. Our value of $\mu_{eff} = 2.7\mu_B$ is much larger than the expected $\mu_{eff} = 1.73\mu_B$ ($C = 0.375$ emu K/mol) for $S = 1/2$. Thus, the $\chi_{dc}(T)$ results ask for a different approach including the effects of charge disproportionation[2] and the contribution of the excited levels of the Ni ions. We will discuss this issue after the analysis of the ESR results.

In Fig. 3 we show ESR spectra taken at different temperatures. The spectrum is observed between 145 K and 560 K and, for $T > T_N$, consists of a single Lorentzian line with $g = 2.16(2)$. This value for the g factor suggests[11] that the resonance species is Ni^{2+}. In Fig. 4 we plot ΔH_{pp} vs T. In the range $T_N < T < 450$ K the linewidth increases with a linear dependence $\Delta H_{pp}(T) = a + bT$ with $a \approx 1300$ G and b

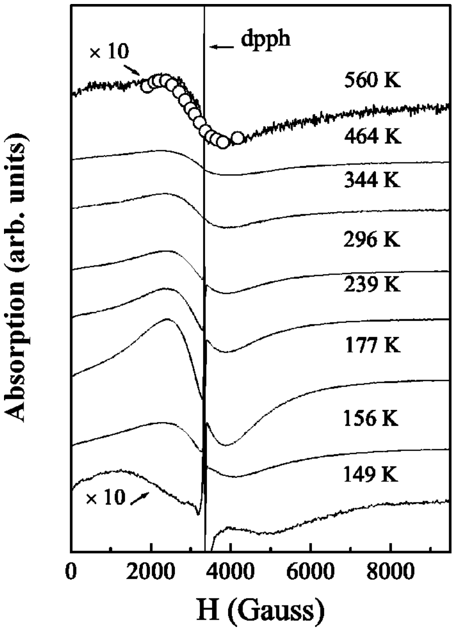

FIG. 3. ESR spectra at different temperatures. For $T=560$ K, the open circles show the central part of the spectrum after subtraction of cavity background. The spectrum of dpph (dyphenil pycril hydrazil) is a marker for $g=2.0036$. The spectra for $T=149$ K and 560 K were amplified 10 times (×10).

≈ 1.5 G/K. Above 450 K some narrowing of the linewidth is observed. A linear dependence for $\Delta H_{pp}(T)$ vs T is characteristic of Ni^{2+} ions, as is discussed in Ref. 12 for the cubic perovskite $\mathrm{KNiF_3}$, where a linear dependence was found above $T \cong 1.4T_N$. In $\mathrm{KNiF_3}$, a crossover to a critical behavior takes place at this temperature and, in the range $T_N < T < 1.4T_N$, $\Delta H_{pp}(T)$ narrows with a dependence $(T-T_N)^{\alpha}$ with $\alpha \cong 1.1$, as in the case of $\mathrm{RbMnF_3}$.[12,13] This kind of critical behavior is observed only in compounds where the magnetic lattice has sc or bcc cubic symmetry.[14] Otherwise, including the case of fcc cubic lattices, a critical broadening ($\alpha < 0$) is measured.[14] In the case of $\mathrm{YNiO_3}$, below $T \approx 1.3T_N$, $\Delta H_{pp}(T)$ abandons the linear dependence and tends to broaden up (see Fig. 3). Since in the perovskite structure the Ni ions are arranged in an approximately sc cubic lattice, the broadening observed may be an indication that not all the Ni contribute to the resonance, besides the effects arising from the small monoclinic distortion. We will return to this point later in connection with the ESR intensity measurements. Notice that, for $T \leqslant T_N$, a different broadening effect is expected for polycrystalline samples.[15] In these cases the splitting of the PM mode into several anisotropic branches and the opening of a T-dependent energy gap combine to give progressively broader inhomogeneous linewidths and lower intensity spectra that are finally lost within the noise, in agreement with our observation (see Fig. 3). Then, the maximum of χ_{ESR} establishes that the resonant Ni ions order AFM below T_N in coincidence with the dc susceptibility peak.

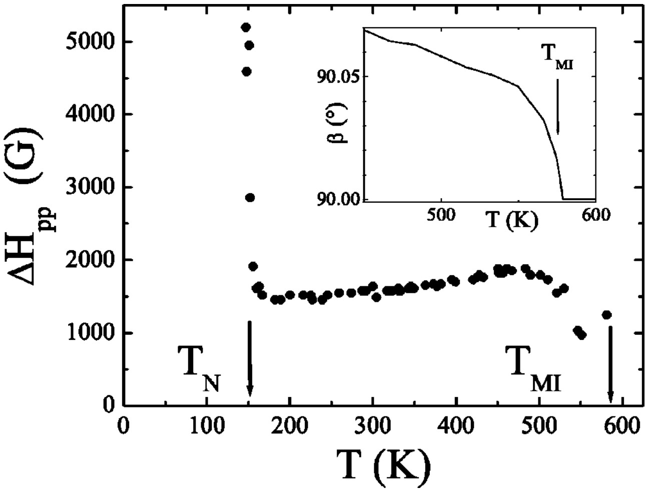

FIG. 4. Temperature dependence of the linewidth $\Delta H_{pp}(T)$. Inset: monoclinic angle $\beta(T)$ vs T from Ref. 2.

In Fig. 2 we show that $\chi_{ESR}(T)$ decreases continuously with T in the whole range 150–560 K and vanishes around 600 K. The disappearance of the ESR line is coincident with the transition observed[2] at $T_{MI}=582$ K. The absence of an ESR spectrum in the metallic phase is compatible with the Ni^{3+} configuration where the e_g electrons are itinerant and the localized t_{2g} electrons have compensated spins. The same behavior (lack of ESR) has been observed[16] for metallic $\mathrm{LaNiO_3}$. A comparison of $\chi_{ESR}(T)$ with $\chi_{dc}(T)$ in the insulating phase shows (see Fig. 2) that χ_{ESR} is, for all temperatures, significantly smaller than χ_{dc}. The ratio χ_{ESR}/χ_{dc} is T dependent: it increases with decreasing T and reaches a value ≈ 0.5 around T_N. The change of behavior across T_{MI} is compatible with a charge disproportionation for $T < T_{MI}$, as proposed in Ref. 2. For a complete disproportionation $2\mathrm{Ni}^{3+} \rightarrow \mathrm{Ni}^{2+} + \mathrm{Ni}^{4+}$, the Ni1 sites would be occupied by Ni^{2+} ($3d^8$) and the Ni2 sites by Ni^{4+} ($3d^6$) ions. Notice that Ni^{4+} is isoelectronic with Co^{3+}, and attempts to observe its ESR spectrum in $\mathrm{LaCoO_3}$ were unsuccessful.[17] The absence of the ESR spectrum may be due to the $S=0$ character of the LS configuration (t_{2g}^6) of Ni^{4+} ions, appropriate for a strong crystal field.[18] Thus, the observed ESR would correspond to the Ni^{2+} in the Ni1 sites.

The proposed disproportionation predicts a Curie constant $C=0.50$ emu K/mol for $\chi_{dc}(T)$ since only half of the Ni ions would contribute as Ni^{2+} ($t_{2g}^6 e_g^2$, $S=1$). This value is significantly smaller than the experimental $C = 0.90(3)$ emu K/mol. On the other hand, if we were to consider the possibility of a high-spin (HS) ground state ($t_{2g}^4 e_g^2$, $S=2$) for Ni^{4+}, as in the free ion, the resulting $C = 2$ emu K/mol would be now much larger than observed. At this point it is then important to analyze the effects of the thermal population of excited states. In order to explain our experimental results we should explore possible states for Ni^{4+} with intermediate-spin (IS) values. Korotin *et al.*[19] have recently calculated the electronic structure for the isoelectronic Co^{3+} in $\mathrm{LaCoO_3}$ and found that the IS configuration ($t_{2g}^5 e_g^1$) with $S=1$ is indeed the first-excited level due to the strong hybridization of $3d$ states with the oxygen $2p$ orbitals. Notice that in a purely ionic picture the HS state is the first-excited level and the IS level is expected to lie at least 1 eV above the ground state.[8] We have calculated $\chi_{dc}(T)$ for an admixture of equal amounts of Ni^{2+} and Ni^{4+} ions. For Ni^{4+} we assumed, as in Ref. 8, that the magnetic contribution arises from a thermally populated IS state lying at an energy Δ above the LS ground state. In this case $\chi_{dc}(T)$ is expected to follow a CW-like law with $C=[C_2+C_4 f(T)]/2$, where $C_2=C_4=1$ emu K/mol correspond to Ni^{2+} and IS Ni^{4+}, respectively, and $f(T)=pe^{-\Delta/k_BT}/(1+pe^{-\Delta/k_BT})$, with p being the degeneracy of the IS excited level.[8] Our observation, for $T>T_N$, of a T-independent $C=0.90(3)$ emu K/mol suggests that $f(T)=0.80(6)$. This is, within the experimental uncertainty, consistent with a value of $\Delta/k_B \ll T_N$ and a degeneracy $3\leqslant p\leqslant 6$ for the IS state.[8] To complete this picture we may associate χ_{ESR} with the Ni^{2+} susceptibility. Here, the ground state of Ni^{4+} does not contribute to the ESR. On the other hand, the excited states are expected to present very short relaxation times (large linewidth) due to the strong phonon modulation of the crystalline field.[20] Then, the corresponding ESR signal would have a very low amplitude, which would be lost within the noise and not included in our line integration. According to our calculation the ratio χ_{ESR}/χ_{dc} would be slightly larger than 0.50, close to our findings for the lowest PM temperatures. Our interpretation of the experiments is then in agreement with the existence of two different Ni sites in the monoclinic structure, occupied by Ni^{2+} and Ni^{4+} ions. The T dependence of χ_{ESR}/χ_{dc} suggests a strong correlation of the spin distribution with the monoclinic distortion, parametrized by the angle $\beta(T)$ shown in the inset of Fig. 4. This correlation is consistent with the decrease of $\Delta H_{pp}(T)$ for $T\geqslant 450$ K since the ESR narrowing may be a consequence of the increase of the site symmetry.[21] The variation of $\chi_{ESR}(T)/\chi_{dc}(T)$ is associated, in this picture, with a progressive disproportionation as T is lowered (and β increases) below T_{MI}.

If the observed CW temperature $\Theta=-310(15)$ K were dominated by first-neighbor interactions—i.e., between Ni1 and Ni2 sites—the predicted AFM order at T_N would be of the G type, contrary to the neutron diffraction results.[2] The order proposed in Ref. 2 implies the division of the system into two fcc interpenetrated lattices of Ni1 and Ni2 sites and has been suggested that Ni1-Ni1 interactions are essential for the stabilization of the magnetic structure,[2,22] due to the less magnetic character of Ni2 sites.[2] The proposed AFM order[2] of the Ni1 sublattice corresponds to the second kind described by Smart[23] for a fcc lattice. In this case, $T_N=-8J_2/k_B$ and $\Theta=(16J_1+8J_2)/k_B$. From the experimental Θ and T_N, AFM exchange constants $J_1/k_B=-10(1)$ K and $J_2/k_B=-19(1)$ K are deduced for first and second Ni1-Ni1 neighbors, respectively. In this kind of ordering the effective field due to first neighbors cancels out and the magnetic structure is stabilized by second neighbors. This interaction corresponds schematically to the Ni^{2+}-O^{2-}-Ni^{4+}-O^{2-}-Ni^{2+} path and may represent an effective AFM interaction favored by the strong hybridization of Ni $3d$ and O $2p$ orbitals.[24]

Finally, we may analyze $\chi_{dc}(T)$ in the orthorhombic metallic phase, where all Ni sites are equivalent. The T-independent susceptibility in $LaNiO_3$ has suggested that in this phase the Ni^{3+} ions are in the LS ground state $t_{2g}^6 e_g^1$ with the e_g electrons fully delocalized. A similar behavior was proposed for $NdNiO_3$, after subtraction of the large Nd contribution.[25] However, in the case of $SmNiO_3$, a CW-like Ni susceptibility was deduced[26] for the metallic phase as in our case ($YNiO_3$), although with a smaller effective magnetic moment ($\mu_{eff}\approx 1.5\mu_B$). It is interesting to revisit here the behavior of $\chi_{dc}(T)$ for the $La_{1-x}Eu_xNiO_3$ series[27] where a transition from a T-independent to a CW-like susceptibility was observed as a function of x. Up to $x\simeq 0.4$, $\chi_{dc}=\chi_0$ and, for larger values of x, a CW component becomes increasingly important. If we look at the phase diagram of Fig. 1, we find that the transition from a T-independent to a CW-like susceptibility occurs in a relatively narrow region around $r_R\simeq 1.1$ Å. This evolution suggests that, for smaller r_R radii, the thermal excitations of electronic configurations with $S\neq 0$ become important also in the metallic phase. This observation reminds the calculations of Korotin *et al.*[19] who found that the relative energies of the different electron configurations of Co^{3+} in $LaCoO_3$ are strongly dependent on the lattice volume. A similar situation may be present for the case of Ni^{3+} in the $RNiO_3$ series. Thus, a calculation of the electronic structure of $RNiO_3$ for different spin states would be worthwhile.

In summary, we have studied the PM properties of the Ni lattice in $YNiO_3$. In the metallic phase, at variance with $LaNiO_3$, we observed a T-dependent susceptibility and we associate this behavior with the small Y^{3+} ionic radius. In the insulating phase, we have observed that Ni ions become resonant and the characteristics of the ESR spectrum correspond to Ni^{2+}. The ESR integrated intensity indicates that only a portion of the Ni ions are observed. Our results are consistent with a charge disproportionation of the type $2Ni^{3+}\rightarrow Ni^{2+}+Ni^{4+}$, accompanying the MI transition, possibly incomplete and T dependent. In this description the Ni^{4+} ions contribute to χ_{dc} through thermally excited configurations but are not detected by ESR techniques.

ACKNOWLEDGMENTS

We acknowledge J. Rodríguez-Carvajal and B. Alascio for helpful comments. This work was partially supported by ANPCyT Argentina (Grant No. PICT 03-05266) and by the Ministry of Science and Technology of Spain (Grant No. MAT2001-0539). R.D.S. and M.T. are CONICET (Argentina) researchers.

---

*Corresponding author. Electronic address: causa@cab.cnea.gov.ar

[1] J.B. Torrance, P. Lacorre, A.I. Nazzal, E.J. Ansaldo, and Ch. Niedermayer, Phys. Rev. B **45**, R8209 (1992) and references therein.

[2] J.A. Alonso, J.L. García-Muñoz, M.T. Fernández-Díaz, M.A.G. Aranda, M.J. Martínez-Lope, and M.T. Casais, Phys. Rev. Lett. **82**, 3871 (1999).

[3] G. Demazeau, A. Marbeuf, M. Pouchard, and P. Hagenmuller, J.

Solid State Chem. **3**, 582 (1971).

[4] J.A. Alonso, M.J. Martínez-Lope, M.T. Casais, J.L. García-Muñoz, and M.T. Fernández-Díaz, Phys. Rev. B **61**, 1756 (2000).

[5] R.D. Sánchez, M.T. Causa, J. Sereni, M.J. Sayagués, M. Vallet-Regí, and J.M. González Calbet, J. Alloys Compd. **191**, 287 (1993).

[6] C. P. Poole, Jr., *Electron Spin Resonance* (Wiley, New York, 1967).

[7] G.F. Goya, R.C. Mercader, L.B. Steren, R.D. Sánchez, M.T. Causa, and M. Tovar, J. Phys.: Condens. Matter **8**, 4519 (1996).

[8] C. Zobel, M. Kriener, D. Bruns, J. Baier, M. Grüniger, T. Lorenz, P. Reutler, and A. Revcolevschi, Phys. Rev. B **66**, 020402 (2002).

[9] K. Sreedhar, J.M. Honig, M. Darwin, M. McElfresh, P.M. Shand, J. Xu, B.C. Crooker, and J. Spalek, Phys. Rev. B **46**, 6382 (1992).

[10] M. Tovar, M.T. Causa, A. Butera, J. Navarro, B. Martínez, J. Fontcuberta, and M.C.G. Passeggi, Phys. Rev. B **66**, 024409 (2002).

[11] The g factor for Ni^{2+} is $g=2.0023-\lambda/\Delta$ (see Ref. 18). The value $g=2.16$ is obtained using $\lambda=-242\ \mathrm{cm}^{-1}$ and $\Delta=12\,000\ \mathrm{cm}^{-1}$ estimated from Ni^{2+} in diamagnetic oxides.

[12] M.T. Causa and M.C.G. Passeggi, Phys. Lett. **98A**, 291 (1983) and references therein.

[13] D.L. Huber, Phys. Lett. **37A**, 283 (1971).

[14] M.S. Seehra and D.L. Huber, in *Magnetism and Magnetic Materials—1974*, edited by C.D. Graham, Jr., G.H. Lander, and J.J. Rhyne, AIP Conf. Proc. No. 24 (AIP, New York, 1975), p. 241; M.S. Seehra and T.G. Castner, Solid State Commun. **8**, 787 (1970).

[15] J.J. Stickler and G.S. Heller, J. Appl. Phys. **33** Suppl., 1302 (1962); E.A. De Meo and G.S. Heller, *ibid.* **37**, 1130 (1966).

[16] R. D. Sánchez, Ph.D. thesis, Instituto Balseiro, San Carlos de Bariloche, Argentina, 1992.

[17] R. D. Sánchez, R. Carbonio, and C. Rettori (private communication).

[18] A. Abragam and B. Bleaney, *Electron Paramagnetic Resonance of Transition Ions* (Clarendon Press, Oxford, 1970).

[19] M.A. Korotin, S.Yu. Ezhov, I.V. Solovyev, V.I. Anisimov, D.I. Khomskii, and G.A. Sawatzky, Phys. Rev. B **54**, 5309 (1996).

[20] D.L. Huber and M.S. Seehra, J. Phys. Chem. Solids **36**, 723 (1975).

[21] M. Tovar, G. Alejandro, A. Butera, A. Caneiro, M.T. Causa, F. Prado, and R.D. Sánchez, Phys. Rev. B **60**, 10 199 (1999).

[22] M.T. Fernández-Díaz, J.A. Alonso, M.J. Martínez-López, M.T. Casais, and J.L. García Muñoz, Phys. Rev. B **64**, 144417 (2001).

[23] J. S. Smart, *Effective Field Theories of Magnetism* (Saunders, Philadelphia, 1966).

[24] S. Yamamoto and T. Fujiwara, cond-mat/0105010 (unpublished).

[25] J. Pérez, J. Stankiewicz, J. Blasco, M. Castro, and J. García, J. Phys.: Condens. Matter **8**, 10 393 (1996).

[26] J. Pérez-Cacho, J. Blasco, J. García, M. Castro, and J. Stankiewicz, J. Phys.: Condens. Matter **11**, 405 (1999).

[27] R.D. Sánchez, M.T. Causa, A. Seoane, J. Rivas, J.F. Rivadulla, M.A. López-Quintela, and J.J. Pérez Cacho, J. Solid State Chem. **151**, 1 (2000).